

REPORT DOCUMENTATION PAGE

AD-A232 035

2

Public reporting burden for this collection of information is estimated to average 1 hour per response, including gathering and maintaining the data needed, and completing and reviewing the collection of information, collection of information, including suggestions for reducing this burden, to Washington Headquarters Operations, Suite 1204, Arlington, VA 22202-4302, and to the Office of Management and Budget, Paperwork Reduction Project (0707-0188), Washington, DC 20503.

1. AGENCY USE ONLY (Leave blank)		2. REPORT DATE		3. REPORT TYPE AND DATES COVERED	
				Annual Report 15 Sep 89-14 Sep 90	
4. TITLE AND SUBTITLE				5. FUNDING NUMBERS	
Optoelectronic III-V Heterostructures on Si Substrates				AFOSR-89-0513	
6. AUTHOR(S)					
Gary Y. Robinson					
7. PERFORMING ORGANIZATION NAME(S) AND ADDRESS(ES)				8. PERFORMING ORGANIZATION REPORT NUMBER	
Colorado State University Dept of Electrical Engineering Fort Collins, CO 80523				AFOSR-TR-91 0019	
9. SPONSORING/MONITORING AGENCY NAME(S) AND ADDRESS(ES)				10. SPONSORING/MONITORING AGENCY REPORT NUMBER	
AFOSR/NE Bldg 410 Bolling AFB DC 20332-6448 Maj Gernot S. Pomrenke				2306/B1	
11. SUPPLEMENTARY NOTES					
<p>DTIC S ELECTE D B FEB 19 1991</p>					
12a. DISTRIBUTION/AVAILABILITY STATEMENT				12b. DISTRIBUTION CODE	
UNLIMITED					
<p>DISTRIBUTION STATEMENT A Approved for public release Distribution Unlimited</p>					
13. ABSTRACT (Maximum 200 words)					
<p>The objective of this research program is to investigate the epitaxial growth and properties of heterostructures of the III-V semiconductors, particularly the InGaAsP/InP system, on Si substrates. The heterostructures are being grown by gas-source molecular beam epitaxy (GSMBE), a technique which have previously used to produce high performance optoelectronic devices using lattice-matched InGaAs/InP and InGaAsP/InP heterostructures and to grow high quality InP layers on Si wafers. The research is focused on exploring methods to reduce misfit dislocations and thus achieve InGaAsP/InP heteroepitaxial materials suitable for high quality optoelectronic devices on Si substrates. InP and lattice-matched InGaAsP alloys are the primary material for high speed optoelectronic telecommunication systems, and an InP-on-Si materials technology would enable VLSI photonics to become a reality.</p>					
14. SUBJECT TERMS				15. NUMBER OF PAGES	
				16. PRICE CODE	
17. SECURITY CLASSIFICATION OF REPORT		18. SECURITY CLASSIFICATION OF THIS PAGE		19. SECURITY CLASSIFICATION OF ABSTRACT	
UNCLASS		UNCLASS		UNCLASS	
				20. LIMITATION OF ABSTRACT	
				UL	

Annual Technical Report

(Covering 15 September 1989 - 14 September 1990)

for

AFOSR Contract #89-0513
Duration: 15 September 1989 - 14 September 1992
USAF Office of Scientific Research
Bolling AFB, DC 20332-6448

entitled

"Optoelectronic III-V Heterostructures on Si Substrates"

performed at

Department of Electrical Engineering
Colorado State University
Fort Collins, CO 80523

PI: Gary Y. Robinson
Office (303) 491-6575
FAX: (303) 491-2249
BITNET: ROBINSON@CSUGREEN.UCC.COLOSTATE.EDU

Annual Technical Report

First Year: 15 September 1989 - 14 September 1990

"Optoelectronic III-V Heterostructures on Si Substrates"

I. RESEARCH OBJECTIVE:

The objective of this research program is to investigate the epitaxial growth and properties of heterostructures of the III-V semiconductors, particularly the InGaAsP/InP system, on Si substrates. The heterostructures are being grown by gas-source molecular beam epitaxy (GSMBE), a technique which we have previously used to produce high performance optoelectronic devices using lattice-matched InGaAs/InP and InGaAsP/InP heterostructures and to grow high quality InP layers on Si wafers. The research is focused on exploring methods to reduce misfit dislocations and thus achieve InGaAsP/InP heteroepitaxial material suitable for high quality optoelectronic devices on Si substrates. InP and lattice-matched InGaAsP alloys are the primary material for high speed optoelectronic telecommunication systems, and an InP-on-Si materials technology would enable VLSI photonics to become a reality. Furthermore, an InP-on-Si technology has applications in light weight, radiation hard InP solar cells for space-borne systems and for III-V optoelectronic devices operating at wavelengths (i.e., $\lambda > 1.2$ microns) requiring a transparent substrate or monolithic waveguides.

In addition to systematically studying the conditions for optimum GSMBE growth, extensive optical, electrical, and structural characterization of the epitaxial films is being carried out in order to assess their suitability for device applications. Collaboration with other researchers included transmission electron microscopy (TEM) analysis by M. M. Al-Jassim at the Solar Energy

Research Institute and mobility profiling by J. P. Lorenzo at the Air Force Rome Air Development Center.

II. MAJOR ACCOMPLISHMENTS:

- * Established the range of controlled p-type and n-type doping in InP-on-Si films and determined mobility variation with depth.
- * Reported the first direct measurement of the band offset energies for the InGaP/GaAs heterojunction.

III. PUBLICATIONS OF WORK SUPPORTED BY THE CONTRACT:

(Total number of publications during this period: 12)

1. T. E. Crumbaker, H. Y. Lee, M. J. Hafich, G. Y. Robinson, M. M. Al-Jassim, and K. M. Jones, "Heteroepitaxy of InP on Si: Reduction of Defects by Substrate Misorientation and Thermal Annealing," J. Vac. Sci. Technol. B 8 (2), 261 (Mar/April 1990).
2. T. E. Crumbaker, M. J. Hafich, G. Y. Robinson, A. Davis, and J. P. Lorenzo, "Heteroepitaxy on Si: Variation of Electron Concentration and Mobility with Depth," Proceedings of the Second International Conference on Indium Phosphide and Related Materials, IEEE LEOS Publications, 1990.
3. J. Chen, J. R. Sites, I. L. Spain, M. J. Hafich, and G. Y. Robinson, "The Band Offset of GaAs/InGaP," submitted to Appl. Physics Letters, June 1990.
4. M. A. Haase, M. J. Hafich, and G. Y. Robinson, "Internal Photoemission and Energy Band Offsets in GaAs-GaInP PIN Heterojunctions," submitted to Appl. Phys. Letters, August 1990.

IV. CONFERENCE PRESENTATIONS OF WORK SUPPORTED BY THIS CONTRACT:

(Total number of presentations during this period: 14)

1. M. J. Hafich and G. Y. Robinson, "Gas-Source MBE Technology for Growth of III-V Heterostructures," 36th National Symposium of the National Vacuum Society, Boston, MA, October 1989.
2. T. E. Crumbaker, M. J. Hafich, G. Y. Robinson, A. Davis, and J. P. Lorenzo, "Heteroepitaxy on Si: Variation of Electron Concentration and Mobility with Depth," Second International Conference on Indium Phosphide and Related Materials, Denver, April 1990.
3. G. A. Patrizi, D. G. Wu, M. J. Hafich, H. Y. Lee, P. Silvestre, and G. Y. Robinson, "Quantum-Confined Stark Effect in InGaP/GaAs Multiple Quantum Wells," Electronic Materials Conference, Santa Barbara, June 1990.

V. INVITED PRESENTATIONS TO INDUSTRY:

1. G. Y. Robinson, "Quantum Well Heterostructures," ATT Bell Laboratories, Allentown, October 1989.



For	
I	<input checked="" type="checkbox"/>
1	<input type="checkbox"/>
on	<input type="checkbox"/>

Availability Codes	
Dist	Avail and/or Special
A-1	

2. G. Y. Robinson, "Gas-Source MBE," short course (video tape) on MBE and MOCVD-New Structures and Devices, IEEE International Electron Devices Meeting, Washington, DC, December 1989.

VI. PERSONNEL

Gary Y. Robinson, Principal Investigator
Mike J. Hafich, Research Associate
Todd E. Crumbaker, Graduate Student, Ph.D. (Physics) May 1991
A. Nanda, Graduate Student, MS (EE) May 1991
Timothy Vogt, Graduate Student, MS (EE) May 1992

VII. RESEARCH RESULTS:

InP on Si

Under previous AF sponsorship, we had reported the first growth of InP on Si by MBE. During the first year of this contract we have endeavored to improve the quality of the InP films and to determine the electrical properties of InP films grown on Si using strained layer superlattice of InGaP/InP as a buffer layer.

A detailed description of our InP-on-Si research is provided in the attached reprints. In summary we found that the unintentionally doped GSMBE films were n-type with carrier concentrations of $(5-10) \times 10^{15} \text{ cm}^{-3}$ and had mobilities of $\mu_{300} = 1000-2000 \text{ cm}^2/\text{v-s}$. Intentional n-type doping with Si was achieved from 5×10^{15} to $5 \times 10^{18} \text{ cm}^{-3}$ and p-type doping with Be from 5×10^{17} to $8 \times 10^{18} \text{ cm}^{-3}$. Profiles of electron concentration for n-type samples showed little variation with depth. Mobility profiles of n-type films, however, showed very low mobility for the first $2 \mu\text{m}$ of growth followed by steadily increasing mobility up to $5.5 \mu\text{m}$, the thickest film grown to date.

InGaAs on Si

During the first year of the contract we have also examined the growth of InGaAs films on Si substrates using InP as an intermediate layer. Previously, we have grown many lattice-matched $\text{In}_{0.53}\text{Ga}_{0.47}\text{As}/\text{InP}$ heterostructures on InP

substrates, including single quantum wells as narrow as 6Å and multiple quantum wells with over 130 periods, that were of very high quality and which provided material for fabrication of high performance optoelectronic devices. Under the sponsorship of this contract, we are attempting to transfer the lattice-matched InGaAs/InP technology to the lattice-mismatched Si substrates.

Our first InGaAs-on-Si samples consisted of a (100) Si substrate misoriented 4° toward the [011] direction, a buffer layer of four $\text{In}_x\text{Ga}_{1-x}\text{P}/\text{In}_y\text{Ga}_{1-y}\text{P}$ ($x \neq y$) strained-layer superlattices, a intermediate layer of InP of 3.0μm in thickness, and a undoped $\text{In}_{0.53}\text{Ga}_{0.41}\text{As}$ film of 2.0μm in thickness. The samples grown to date exhibited spotty high energy electron diffraction patterns during growth and poor surface morphology after growth, clear indications that optimum growth conditions have not yet been achieved for growth of InGaAs on Si wafers. Apparently the indicated substrate temperature for the three-inch diameter Si wafers in our MBE system is greatly different than the substrate temperature obtained during growth on the much smaller InP wafers, and the substrate temperature is more critical in the growth of InGaAs than InP. Experiments are currently underway to calibrate the Si substrate temperature.

We have recently found that the accumulation of phosphorous on the walls of the growth chamber of our GSMBE system has adversely affected our method of insitu cleaning of Si substrates prior to growth. The Si wafer is introduced into the vacuum system with a carefully prepared thin oxide layer which is normally desorbed at about 800°C, leaving an clean, atomically flat surface for epitaxial growth. However, we now find that after about three years of growth of III-V phosphides in our MBE system, the phosphorous from the walls of the system deposits on the surface of the Si wafer to form a tenacious oxide layer that will not desorb even at 1000-1100°C. To overcome this problem, we have

adopted a new method of cleaning the Si surface, first reported by Steve Wright and Herb Kroemer, in which the substrate is held at 800°C while exposed to a Ga molecular beam. Our preliminary results indicate that the Ga reacts with phosphosilicate glass layer to form volatile molecular species which readily desorb, leaving a Si surface suitable for epitaxial growth.

InGaP/GaAs Heterojunction

As noted above, we are using the III-V alloy semiconductor $\text{In}_x\text{Ga}_{1-x}\text{P}$ for a superlattice buffer layer, since by varying the composition x the lattice constant can be varied from that of Si to that of InP. At $x = 0.48$, InGaP is lattice matched to GaAs and InGaP/GaAs heterojunctions are finding an increasing number of applications in visible light emitting devices and in heterojunction bipolar transistors. The values of the conduction band offset energy ΔE_c and valence band offset ΔE_v of the InGaP/GaAs heterojunction are not well established, yet these values are critical to the design of devices employing InGaP/GaAs heterojunctions. We have undertaken two collaborations with researchers in other laboratories to determine the band offsets in our GSMBE InGaP/GaAs material. Both collaborations have resulted in new results which indicate the value for ΔE_c is much lower than previously believed, making the InGaP/GaAs heterojunction attractive for new device applications in optoelectronics. One such device is an InGaP/GaAs MQW optical modulator where the smaller value of ΔE_c offers the advantage of a larger quantum-confined Stark shift than in conventional AlGaAs/GaAs modulators. We recently presented this new approach at a conference and an abstract is attached.

The first collaboration was with workers in the Physics Department at Colorado State who are experts in measuring the change in the bandstructure of semiconductors under very large hydrostatic pressures. Using multiple quantum

well InGaP/GaAs samples grown in our laboratory they have determined the valence band offset ΔE_v to be 0.40 ± 0.02 eV, and hence a $\Delta E_c = 0.06 \pm 0.02$ eV. A manuscript which has been submitted for publication is attached.

The second collaboration was with Michael Haase of the 3M Company, who used internal photoemission to determine the band offset energy in a InGaP/GaAs pin heterojunction photodiode grown in our laboratory. Analysis of the photocurrent data indicate a $\Delta E_c = 108 \pm 6$ meV, somewhat higher than the high pressure results but still well below previously published values. Attached is a paper describing the details of the research.

VII. FUTURE WORK

We plan to continue our studies of the growth of InGaAs on Si substrates. The optimum substrate temperature and V/III ratio will be determined. The quality of the InGaAs layers will be determined by TEM, photoluminescence, X-ray diffraction, and electrical measurements. Next, quantum well InGaAs/InP structures will be grown and the degree of quantum confinement will be determined. These experiments should provide the basis for a preliminary evaluation of the suitability of InGaAs-on-Si for optoelectronics devices.

We also plan to examine the mechanism of GSMBE growth of III-V materials. We plan to conduct experiments where unwanted carbon incorporation may be inhibited by the presence of uncracked hydride molecular species on the film surface during growth. Preliminary results indicate a reduction in C incorporation during GSMBE growth of GaAs using partially cracked AsH_3 . If successful, this effect may be a significant advantage of the GSMBE growth technique.

Heteroepitaxy of InP on Si: Reduction of defects by substrate misorientation and thermal annealing

T. E. Crumbaker, H. Y. Lee, M. J. Hafich, and G. Y. Robinson

Department of Electrical Engineering and the Center for Optoelectronic Computing Systems, Colorado State University, Fort Collins, Colorado 80523

M. M. Al-Jassim and K. M. Jones

Solar Energy Research Institute, Golden, Colorado 80401

(Received 13 September 1989; accepted 5 October 1989)

The results of a study of the effects of substrate misorientation and *ex situ* thermal annealing on the morphology, defect density, and low temperature photoluminescence (PL) emission of epitaxial films of InP grown on Si substrates are presented. InP films were grown by gas-source molecular beam epitaxy on both (100) oriented and (100) misoriented 4° towards the [011] Si wafers. InP films on misoriented substrates were mirror-like over the entire 3-in. wafer and exhibited a factor of 2 lower dislocation density than films on oriented substrates, as determined by double crystal x-ray diffraction and transmission electron microscopy (TEM). Thermal annealing resulted in a significant enhancement of the low temperature near band edge PL emission and a decrease in the density of dislocations and stacking faults. The best results obtained were for annealed films on misoriented substrates with an x-ray linewidth of 440 arcsecs, a TEM dislocation density of $\sim 2 \times 10^8 \text{ cm}^{-2}$, a stacking fault density of $\sim 2 \times 10^7 \text{ cm}^{-2}$, and a PL linewidth of 6 meV.

I. INTRODUCTION

Increasing interest has been given to the growth of InP on Si despite the 8% lattice mismatch of this material system. Besides providing large area substrates for III-V growth, monolithic integration of InP and related compounds with Si would allow the combining of optical sources, modulators, and detectors operating at 1.3 and 1.55 μm with Si integrated circuits. The growth of large area epitaxial InP films on Si substrates has been reported by metalorganic chemical vapor deposition (MOCVD)¹⁻⁴ and molecular beam epitaxy (MBE),^{5,6} and MOCVD has recently been used to produce InP/Si solar cells⁷ and an InGaAsP/Si laser.⁸ The primary limiting factor in device performance has been the high defect density in the films due to misfit dislocations caused by the large lattice mismatch. The use of misoriented substrates and thermal annealing for GaAs films grown on Si resulted in a substantial reduction in defect density.^{9,10} Here, we report the results of an investigation of the effects of substrate orientation and *ex situ* thermal annealing on the properties of InP-on-Si films grown by gas-source MBE.

II. EXPERIMENTAL PROCEDURE

Three-inch diameter *p*-type Si substrates of 10-20 $\Omega \text{ cm}$ resistivity were etched in $5\text{H}_2\text{SO}_4:1\text{H}_2\text{O}_2$, then transferred to a N_2 atmosphere and etched in a $\text{HF}:\text{H}_2\text{O}$ solution before being loaded into the MBE system. Both (100) oriented and (100) misoriented 4° towards the [011] wafers were used. The substrates were cleaned *in vacuo* at 700-1000 $^\circ\text{C}$ for 20 min prior to growth. Gas-source MBE was used to grow the heterostructures with the In and Ga beams provided by conventional effusion cells and a P_2 beam produced by thermal decomposition of gaseous PH_3 at 900 $^\circ\text{C}$ in a low-pressure cracking oven.¹¹ The Si surface was first exposed to the P_2

beam for a brief period at 300 $^\circ\text{C}$, then a GaP layer of approximately 0.04 μm in thickness was grown at 0.1-0.6 $\mu\text{m}/\text{h}$, followed by a buffer layer consisting of four strained layer superlattices of $\text{In}_x\text{Ga}_{1-x}\text{P}/\text{In}_y\text{Ga}_{1-y}\text{P}$ ($x \neq y$) described previously.⁵ The buffer layer was then capped with an undoped InP active layer of 4 μm thickness grown at 480 $^\circ\text{C}$ and 1 $\mu\text{m}/\text{h}$. Reflection high energy electron diffraction (RHEED) patterns were observed during growth.

After growth, thermal annealing of the InP-on-Si wafers was performed in an open tube furnace with a N_2 gas flow of 1 sccm at temperatures of 600-900 $^\circ\text{C}$ for 3 to 1000 min. To prevent loss of phosphorus from the InP films at the high temperatures, the InP-on-Si wafers were capped with 50-100 nm of SiO_2 , chemically vapor deposited at 250 $^\circ\text{C}$,¹² and a bare InP wafer was placed on the SiO_2 surface to provide a source of phosphorus overpressure during annealing. Both the as-grown and annealed films were characterized by Nomarski microscopy, surface profilometry, double crystal x-ray diffraction, low temperature photoluminescence, and transmission electron microscopy.

III. RESULTS AND DISCUSSION

A. Oriented versus misoriented substrates

In this section, the effects of substrate orientation on as-grown films are presented. Prior to growth, (2×2) RHEED patterns were observed for both the oriented and misoriented Si substrates after heating to 700-1000 $^\circ\text{C}$. During growth of the InP active layer on both oriented and misoriented substrates, the RHEED pattern was a well-defined P_2 -stabilized (2×4) reconstruction, very similar to that of high-quality homoepitaxial InP grown under identical conditions. However, streaks began to appear near the middle of the growth of the buffer layer on misoriented substrates, but

not until the very end of the buffer layer on oriented substrates. After growth, layers on oriented substrates appeared mirror-like over about 25% of the wafer surface, whereas layers on misoriented substrates were mirror-like over the entire wafer. Nomarski microscopy revealed a slight ripple at high magnification ($1000\times$) for all layers, but the ripple was less pronounced for layers on misoriented substrates. Overall, films on misoriented substrates exhibited the best morphology.

Characterization data comparing InP films on oriented and misoriented Si substrates are summarized in Table I. Data for films on oriented substrates are reported only for the regions of the wafer that were mirror-like; film quality was poor in the non-mirror-like areas. Surface roughness estimated from the average peak-to-peak variation of a surface profilometer trace across the sample surface was 10–12 nm for misoriented substrates but was consistently higher (24–40 nm) for oriented substrates. For comparison, our homoepitaxial InP films have surface roughness below the sensitivity of the profilometer (<2.5 nm).

Using double crystal x-ray (DCXR) diffraction with CuK_α radiation, the full width at half-maximum (FWHM) of the (400) InP peak and the tilt of the InP lattice relative to the Si lattice was determined.⁵ A typical DCXR diffraction spectrum of as-grown InP on a misoriented substrate is shown in Fig. 1(a). Films on oriented substrates had FWHM between 900–1300 arcsecs and were tilted less than 0.5° from the [001] Si direction. Films on misoriented substrates had FWHM between 650–800 arcsecs and were tilted less than 1.0° from the Si lattice along the [011] direction, which corresponds to the direction of misorientation. DCXR FWHM for homoepitaxial InP grown under similar conditions in our MBE system are typically less than 20 arcsecs. The large FWHM for the InP/Si films is indicative of the presence of a large number of dislocations. The following equation from Hirsch¹³ for the dislocation density, $D = 1600^*[\text{FWHM}]^2$, where we have assumed the magnitude of the Burger's vector to be 0.4 nm, can be used to estimate the dislocation density D in cm^{-2} based on the DCXR FWHM in arcsec. This equation was used to calculate the values shown in Table I and yields a dislocation density of 2×10^9 and $9 \times 10^8 \text{ cm}^{-2}$ for films on oriented and misoriented substrates, respectively.

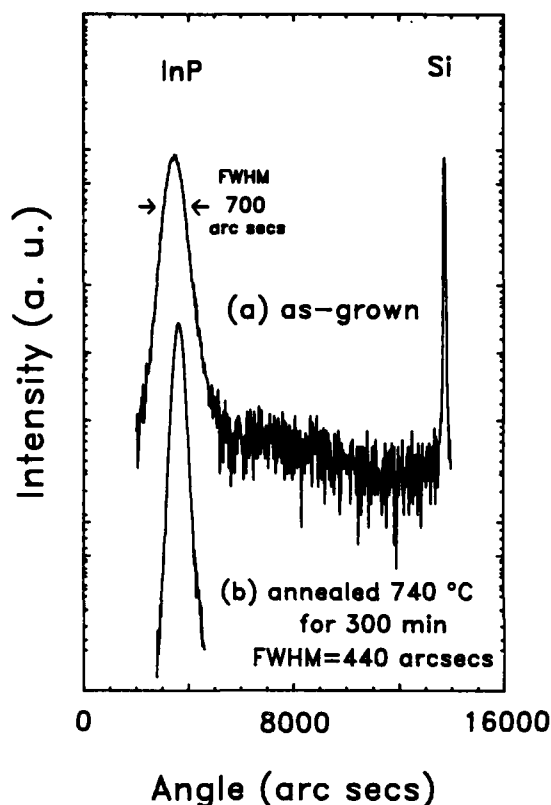


FIG. 1. Double crystal x-ray diffraction spectra for InP grown on a misoriented substrate. (a) As-grown and (b) annealed at 740°C for 300 min.

To complement the x-ray measurements, transmission electron microscope (TEM) measurements were performed using a Phillips CM-30 TEM at 300 keV. Cross-sectional TEM samples were prepared by mechanical polishing followed by iodine ion beam milling. The latter proved to be essential to prevent the loss of phosphorus from the InP. Figure 2 is a TEM cross-section of an InP film on a misoriented substrate; this sample has been annealed but as-grown samples showed similar cross sections. The Si substrate, superlattice (SL) buffer layer, and InP active layer with a large number of threading dislocations and stacking faults are clearly discernible. Furthermore, the density of dislocations are seen to decrease away from the SL buffer layer, with the

TABLE I. Comparison of InP film on oriented and misoriented Si substrates.

Parameter	Oriented Si substrate (as-grown)	Misoriented Si substrate (as-grown)	Misoriented Si substrate (annealed $800^\circ\text{C}/5$ min)
Surface roughness (nm)	24–40	10–12	8–12
DCXR FWHM (arcsecs)	900–1300	650–800	440–560
PL FWHM at 13 K	19–21	8–13	6
Dislocation density (cm^{-2})			
(a) DCXR	$\sim 2 \times 10^9$	$\sim 9 \times 10^8$	$\sim 4 \times 10^8$
(b) TEM	$(7-9) \times 10^8$	$(4-6) \times 10^8$	$(1-3) \times 10^8$
Stacking fault density			
TEM (cm^{-2})	$(4-6) \times 10^8$	$(1-3) \times 10^8$	$(1-3) \times 10^7$

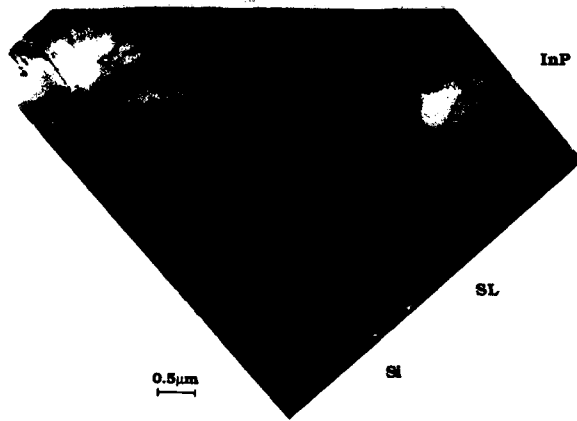


FIG. 2. Transmission electron microscope cross section of an annealed (800 °C for 5 min) InP film on a misoriented substrate.

number of dislocations being much lower in the upper 2 μm of the InP active layer.

Direct measurement of the average threading dislocation and stacking fault densities in regions close to the surface of as-grown InP films was obtained using plan-view TEM micrographs of the type shown in Fig. 3(a) and the results are

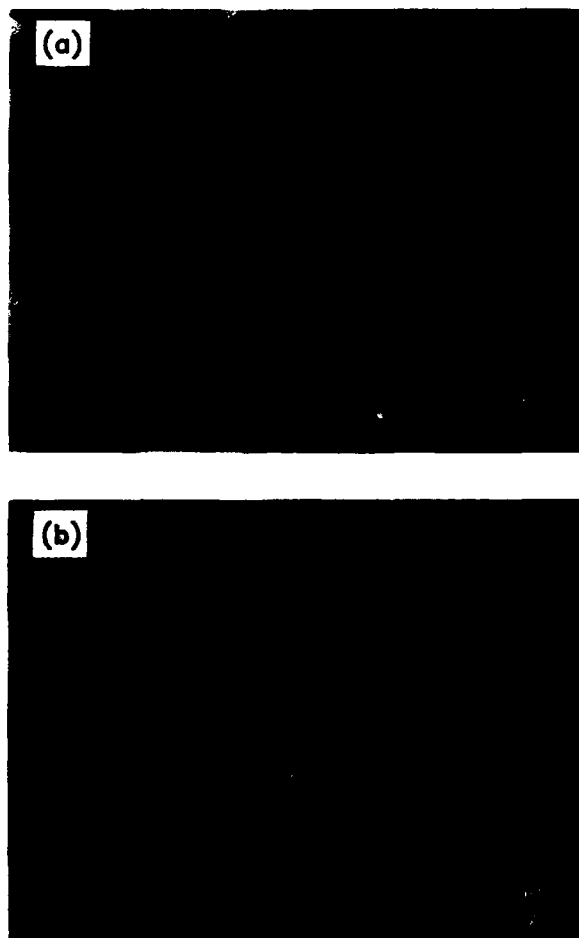


FIG. 3. Plan-view TEM micrographs of an InP film on a misoriented Si substrate. (a) As-grown and (b) annealed at 740 °C for 300 min.

given in Table I. Both the dislocation density and the stacking fault-density were lower by about a factor of 2 for the misoriented substrate. Note that in Table I, the DCXR dislocation density calculated from the Hirsch equation is somewhat higher than actually observed with TEM. The Hirsch equation assumes a uniform density of dislocations with depth,¹³ which from Fig. 2 is clearly not the case here. The x-ray technique averages over the entire volume of the InP film and thus yields a dislocation density higher than that from TEM defect counts made in regions near the top of the InP film.

Photoluminescence (PL) at 10–25 K was performed using Ar⁺ laser excitation at 514 nm, a 0.5-m monochromator, and a Ge detector. The PL spectra for a homoepitaxial InP film and an InP film on an oriented Si substrate are shown in Fig. 4. Both oriented and misoriented InP-on-Si films exhibited three peaks with the near band edge peak at 1.410 eV believed to be the neutral-acceptor-bound-exciton transition, being dominant. Compared with spectra for homoepitaxial InP, the near band edge peak of InP-on-Si films was shifted to lower energy by 4–6 meV, presumably as a result of residual strain in the film. Similar shifts have been observed in InP-on-Si grown by MOCVD.¹ The peaks at 1.37 and 1.33 eV do not correspond to acceptor or donor impurities commonly found in homoepitaxial InP¹⁴ but have been previous-

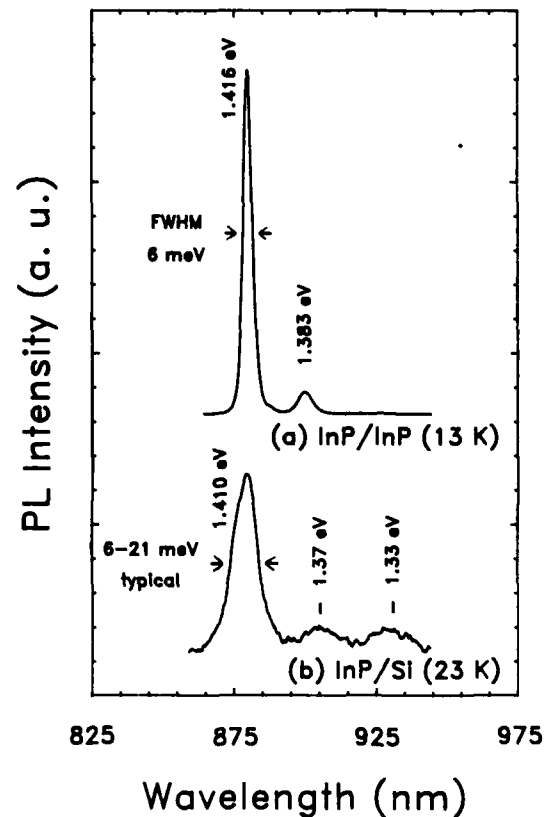


FIG. 4. Photoluminescence spectra for (a) a homoepitaxial InP layer (intensity scale $1\times$), and (b) an InP film on an oriented Si substrate (scale $400\times$). The spectrum for the InP-on-Si film exhibits the three peaks typically found in InP-on-Si films. Both (a) and (b) are for unintentionally doped material which contained a residual donor density of approximately 10^{16} cm^{-3} .

ly observed in InP-on-Si grown by MOCVD.⁷ Thus, the peaks at 1.37 and 1.33 eV appear to be produced by defects resulting from the large InP-Si lattice mismatch. The FWHM of the largest PL peak for misoriented substrates was 8–13 meV and is narrower than for oriented substrates which was 19–21 meV.

B. Thermal annealing

A systematic examination of the effects of *ex situ* thermal annealing was carried out. Typical DCXR spectra are shown in Fig. 1 where the FWHM of an InP film on misoriented Si decreases from 700 to 440 arcsec after an anneal at 740 °C for 300 min. The x-ray linewidth was always found to decrease with annealing and Fig. 5 summarizes the effect of annealing at 600, 700, and 800 °C on an InP film on a misoriented substrate by plotting the FWHM normalized to the as-grown value versus cumulative annealing time. At 900 °C the capping method failed, resulting in a decomposed InP surface. Figure 5 shows that a decrease of approximately 30% in DCXR FWHM was achieved by furnace annealing at 800 °C. The lowest value of FWHM obtained was 440 arcsecs. Using 800 °C for 4 min, the same percentage reduction in DCXR FWHM was observed for films on oriented substrates although the as-grown FWHM value was larger. From Hirsch's equation for dislocation density, a 30% reduction in DCXR FWHM corresponds to a factor of 2 reduction in dislocation density. This was confirmed by direct measurement of the average dislocation density by plan-view TEM as shown in Fig. 3(b). Defect counts of annealed films on misoriented substrates gave a dislocation density of $(1-3) \times 10^8 \text{ cm}^{-2}$ and a stacking fault density of $(1-3) \times 10^7 \text{ cm}^{-2}$. Thus, thermal annealing had the greatest effect on the stacking faults, reducing the stacking fault density an order of magnitude. Similar reduction factors were observed for the defects in annealed films on oriented substrates.

Annealed films using our capping procedure showed no measurable change in surface roughness and no discernible change in morphology as observed by Nomarski micros-

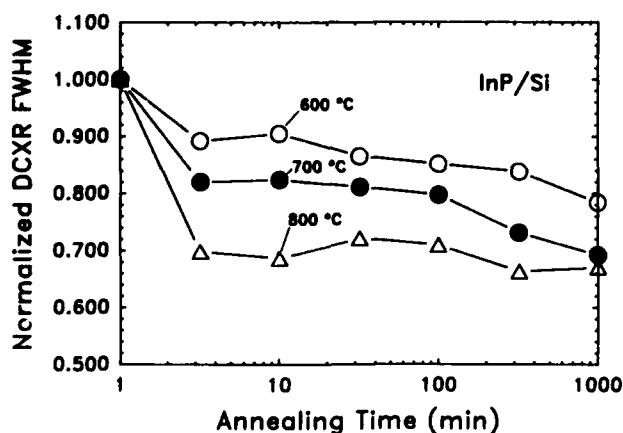


FIG. 5. Normalized double crystal x-ray FWHM for the InP (400) reflection vs cumulative annealing time at three temperatures for a misoriented substrate. The lowest FWHM achieved was 440 arcsecs.

copy. Low temperature PL spectra for as-grown and annealed films on misoriented substrates are shown in Fig. 6. Annealing produces an increase in intensity of the near band edge peak, a smaller FWHM, and a decrease in the intensities of the defect related peaks. The FWHM of 6 meV for the annealed sample is smaller than reported for InP-on-Si by MOCVD¹ and is the same as for our highest quality homoepitaxial InP when measured at 13 K. Table I summarizes the annealing results on misoriented substrates.

IV. CONCLUSIONS

InP films grown on (100) Si substrates misoriented 4° towards [011] exhibited greater morphological uniformity over a 3-in. diameter wafer than films grown on nominally oriented (100) substrates. *Ex situ* thermal annealing at 700–800 °C enhanced the near band edge PL emission from the InP and decreased emission from defect related peaks. And finally, as in the case of GaAs/Si heteroepitaxy, substrate misorientation and thermal annealing both resulted in a substantial reduction in the density of defects in InP films on Si substrates. Annealed InP films on misoriented Si substrates exhibited approximately a factor of 4 reduction in dislocation density and more than an order of magnitude reduction in stacking fault density over as-grown films on nominally oriented substrates.

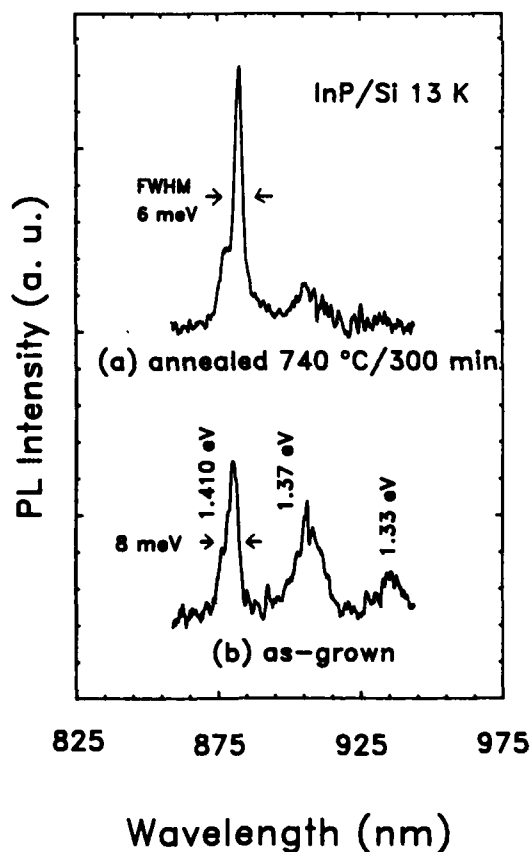


FIG. 6. Photoluminescence spectra for InP on a misoriented substrate. (a) Annealed at 740 °C for 300 min and (b) as-grown. The intensity scale is the same in (a) and (b).

ACKNOWLEDGMENTS

The authors gratefully acknowledge the assistance of D. Williams, R. Iyer, and J. Chen. This work was supported by Air Force-Hanscom (Contract No. F-19628-88-K-0006) and the Air Force Office of Scientific Research (Contract No. F49620-86-K-0021).

¹D. S. Wu, R. H. Horng, K. C. Huang, and M. K. Lee, *Appl. Phys. Lett.* **54**, 236 (1989); D. S. Wu, R. H. Horng, and M. K. Lee, *Appl. Phys. Lett.* **54**, 2244 (1989).

²N. Uchida, M. Suga, A. Yamamoto, and M. Yamaguchi, *Extended Abstracts, 19th Conference on Solid State Devices and Materials* (Japan Society of Applied Physics, Tokyo, 1987), p. 155.

³M. Razeghi, M. Defour, F. Omnes, J. Nagle, P. Maurel, O. Archer, and D. Mijuin, *Heteroepitaxy on Si* (Materials Research Society, Pittsburgh, PA, 1988), *Mater. Res. Soc. Symp. Proc.* Vol. 116, p. 297.

⁴S. J. Pearton, K. T. Short, A. T. Macrander, C. R. Abernathy, V. P. Mazzi, N. M. Haegel, M. M. Al-Jassim, S. M. Vernon, and V. E. Haven, *J. Appl. Phys.* **65**, 1083 (1989).

⁵T. E. Crumbaker, H. Y. Lee, M. J. Hafich, and G. Y. Robinson, *Appl. Phys. Lett.* **54**, 140 (1989).

⁶H. Y. Lee, T. E. Crumbaker, M. J. Hafich, G. Y. Robinson, M. M. Al-Jassim, and K. M. Jones, *Proceedings of the 1st International Conference on InP and Related Materials for Advanced Electronics and Optical Devices*, edited by R. Singh and L. J. Messick (SPIE, Bellingham, WA, 1989), Vol. 1144.

⁷C. J. Keavney, S. M. Vernon, V. E. Haven, S. J. Wojtczuk, and M. M. Al-Jassim, *Appl. Phys. Lett.* **54**, 1139 (1989); S. M. Vernon, V. E. Haven, C. R. Abernathy, S. J. Pearton, A. T. Macrander, V. M. Hagel, V. P. Mazzi, K. T. Short, and M. M. Al-Jassim, *International Symposium on Gallium Arsenide and Related Compounds*, Atlanta, September, 1988.

⁸M. Razeghi, M. Defour, F. Omnes, Ph. Maurel, J. Chazelas, and F. Briouillet, *Appl. Phys. Lett.* **53**, 725 (1988).

⁹R. Fischer, D. Neuman, H. Zabel, H. Morkoc, C. Choi, and N. Otsuka, *Appl. Phys. Lett.* **48**, 1223 (1986).

¹⁰C. Choi, N. Otsuka, G. Munns, R. Houdre, H. Morkoc, S. L. Zhang, D. Levi, and M. V. Klein, *Appl. Phys. Lett.* **50**, 992 (1987).

¹¹M. B. Panish, in *Progress of Crystal Growth and Characteristics*, edited by B. R. Pamplin and R. Z. Bachrach (Pergamon, Oxford, 1986), Vol. 123, pp. 1-28.

¹²R. Iyer and D. L. Lile, *J. Electrochem. Soc.* **135**, 693 (1988).

¹³P. B. Hirsch, in *Progress in Metal Physics*, edited by B. Chalmers and R. King (Pergamon, New York, 1956), Vol. 6, p. 236.

¹⁴B. J. Skromme, G. E. Stillman, J. D. Oberstar, and S. S. Chan, *J. Electron. Mater.* **13**, 463 (1984).

Heteroepitaxy of InP on Si: Variation of Electron Concentration and Mobility with Depth

T.E. Crumbaker, M.J. Hafich, and G.Y. Robinson
Department of Electrical Engineering and
the Center for Optoelectronic Computing Systems
Colorado State University, Fort Collins, CO 80523

and

A. Davis and J.P. Lorenzo
Rome Air Development Center
Solid State Sciences Directorate
Hanscom AFB, MA 01731

ABSTRACT

Electrical properties of InP single crystal films grown by gas-source MBE on Si(100) substrates is described. To accommodate the 8% InP-Si lattice mismatch, a strained-layer superlattice of InGaP was used as a buffer layer. Unintentionally doped films were n-type with carrier concentrations of $(5-10) \times 10^{15} \text{ cm}^{-3}$ and had mobilities of $\mu_{300} = 1000-2000 \text{ cm}^2/\text{v-s}$. Intentional n-type doping with Si was achieved from 5×10^{15} to $5 \times 10^{18} \text{ cm}^{-3}$ and p-type doping with Be from $5 \times 10^{17} \text{ cm}^{-3}$ to $8 \times 10^{18} \text{ cm}^{-3}$. Profiles of electron concentration for n-type samples showed little variation with depth. Mobility profiles of n-type films, however, showed very low mobility for the first $2 \mu\text{m}$ of growth followed by steadily increasing mobility up to $5.5 \mu\text{m}$, the thickest film grown to date.

1. INTRODUCTION

With the advent of a monolithic InP/Si technology, optical sources, detectors, and modulators operating at 1300 and 1550 nm could be fabricated on transparent Si substrates or combined with Si waveguides [1]. Metalorganic chemical vapor deposition (MOCVD) [2-4] and gas-source molecular beam epitaxy (MBE) [5] have been used to grow large area single crystal InP films on Si substrates and Razeghi et. al. [6] has used low pressure MOCVD to produce an InGaAsP/InP laser on Si. We report here the results of n- and p-type dopant incorporation and electron concentration and mobility versus depth for InP-on-Si films grown by gas-source MBE.

2. EXPERIMENTAL PROCEDURE

Three-inch diameter Si substrates were etched in 5:1 $\text{H}_2\text{SO}_4:\text{H}_2\text{O}_2$, then transferred to a N_2 atmosphere and etched in a dilute HF solution before being loaded into the MBE system. For n-type films, p-type Si substrates of 20 ohm-cm resistivity were used and for p-type films, n-type Si wafers of 0.1 ohm-cm were used. Both (100) oriented and (100) misoriented 4° towards the [011] wafers were used. The substrates were cleaned in vacuo at 700-1000 °C for 20 min prior to growth. Gas-source MBE was used to grow the heterostructures with the In and Ga beams provided by conventional effusion cells and a P_2 beam provided by thermal decomposition of gaseous PH_3 at 900 °C in a low pressure cracking oven. Conventional effusion cells were also used for Si and Be beams for n- and p- type doping, respectively. A buffer layer 0.6 μm thick was placed between the Si substrate and InP active layer and consisted of GaP followed by four strained-layer superlattices of $\text{In}_x\text{Ga}_{1-x}\text{P}/\text{In}_y\text{Ga}_{1-y}\text{P}$ ($x \neq y$). Details of this buffer layer have been described elsewhere [5]. The buffer layer was followed by an InP active layer 3.5-5.0 μm thick grown at 480 °C and 0.85 $\mu\text{m}/\text{hr}$.

The carrier concentration was measured by Hall-van der Pauw measurements for n-type films and tungsten (W) probe breakdown measurements for p-type films. W probe breakdown measurements were used for p-type films because of difficulty in obtaining adequate ohmic contacts to p-type InP on Si over a wide range of carrier concentration. The breakdown of W probes on InP was calibrated on several substrates of known carrier concentration.

Depth profiling of Hall mobility and carrier concentration was performed on n-type films by two techniques. Method #1 used anodic layer stripping combined with differential Hall measurements [7]. At each etch step, a 500 Å thick anodic oxide was grown in a glycol and water electrolyte and then removed with dilute HF. Ohmic contacts were made with Au/Ge/Ni. Method #2 used iodic acid etching combined with Hall-van der Pauw measurements. InSn ohmic contacts were protected while 0.5 - 1.0 μm of the sample was etched in a 10:1 H₂O:HIO₃ solution. Bulk mobility and carrier concentration determined from method #1 compared favorably with data of method #2.

3. RESULTS AND DISCUSSION

Unintentionally doped InP-on-Si films are n-type with a residual carrier concentration of (5-10) × 10¹⁵ cm⁻³. Intentional n-type doping with Si was achieved from the residual concentration up to 5 × 10¹⁸ cm⁻³. Intentional p-type doping with Be was achieved from 5 × 10¹⁷ cm⁻³ to 8 × 10¹⁸ cm⁻³. Attempts to p-dope lower than 5 × 10¹⁷ cm⁻³ resulted in a conversion to n-type material.

Depth profiling of the mobility and carrier concentration of two n-type InP-on-Si films were performed and the results are shown in Fig. 1. Sample MBE 195 was 4.0 μm thick and doped at 5 × 10¹⁵ cm⁻³ while sample MBE 141 was 5.5 μm thick with 8 × 10¹⁵ cm⁻³ doping. Method #1 was used to profile entirely through the 4.0 μm sample and through the first 2 μm of the 5.5 μm sample. Both mobility and carrier concentration were normalized to the values obtained before etching in sample 141, resulting in continuity in the data between the two samples at the point 4.0 μm from the Si interface. Fig. 1(a) clearly shows a gradual decrease in mobility with depth until the mobility drops to near zero at 2 μm from the Si interface. Typical mobilities of the 5.5 μm film before etching were in the range 1000-2000 cm²/V-s while InP-on-InP films exhibited electron mobilities of 3500 - 4100 cm²/V-s. Fig. 1(b) shows a slight decrease in carrier concentration versus depth using method #1.

Method #2 was also used on both samples and the results are plotted as solid symbols in Fig. 1. The data for method #2 were normalized the same way as for method #1. The mobility and carrier concentration data of Fig. 1 agree reasonably well by both methods. The large increase in carrier concentration obtained by method #2 at - 1.5 μm from the Si interface is not yet understood. It should be pointed out that the Hall-van der Pauw measurements for this data point were suspect because of nonlinear ohmic contacts. A SIMS profile of Si concentration showed a sharp drop in Si concentration within 0.2 μm of the Si interface. Thus up-diffusion from the Si-substrate does not seem likely.

In conclusion, InP-on-Si films can be controllably doped n- or p-type in a manner similar to homoepitaxial InP material. And although the carrier concentration decreases slightly with depth into the sample, the mobility is very low near the Si interface and slowly increases with increasing film thickness, reaching only 1000 - 2000 cm²/V-s in n-type films of about 5 μm thickness. Since our earlier studies using transmission electron microscopy [5] indicated a corresponding decrease in the densities of threading dislocations and stacking faults away from the Si interface, it appears that lattice-defect scattering dominates the electron mobility in InP-on-Si films.

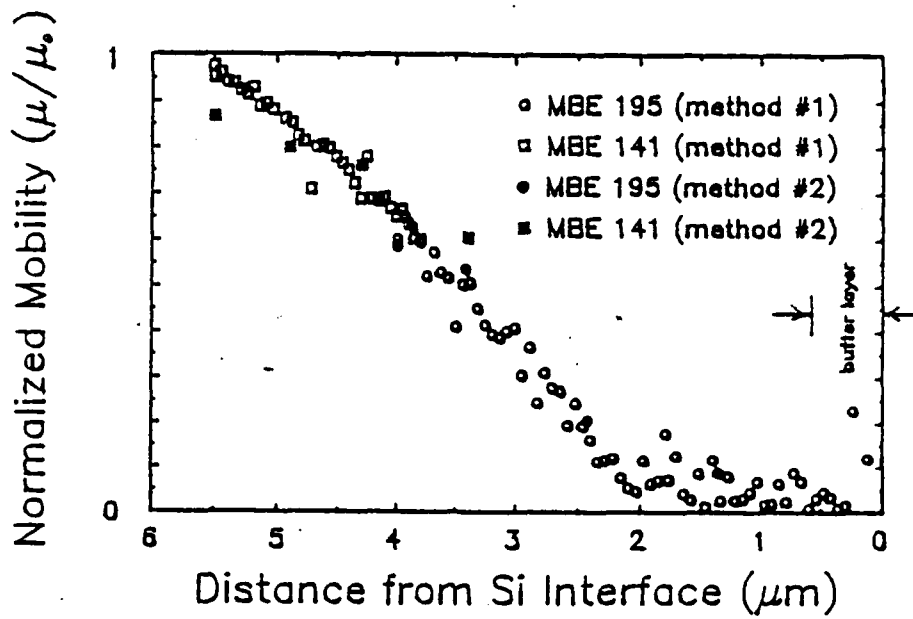
4. ACKNOWLEDGMENTS

The authors gratefully acknowledge the assistance of S. Asher at the Solar Energy Research Institute in Golden, CO for providing the SIMS profiles. This work was supported by Air Force-Hanscom (contract #F19628-88-K-0006) and the Air Force Office of Scientific Research (contract #89-0503).

5. REFERENCES

1. R. A. Soref and J. P. Lorenzo, IEEE Journ. Quantum Electron. QE-22, 873 (1986).
2. M. K. Lee, D. S. Wu, and H. H. Tung, Appl. Phys. Lett. 50, 1725 (1987).
3. M. Razeghi, M. Defour, F. Omnes, J. Nagle, P. Maurel, O. Acher, and D. Mijuin, Heteroepitaxy on Si (Materials Research Society, Pittsburgh, PA, 1988), Mater. Res. Soc. Symp. Proc. Vol. 116, p. 297.
4. S. J. Pearton, K. T. Short, A. T. Macrander, C. R. Abernathy, V. P. Mazzi, N. M. Haegel, M. M. Al-Jassim, S. M. Vernon, and V. E. Haven, J. Appl. Phys. 65, 1083 (1989).
5. T. E. Crumbaker, H. Y. Lee, M. J. Hafich, and G. Y. Robinson, Appl. Phys. Lett. 54, 140 (1989); T. E. Crumbaker, H. Y. Lee, M. J. Hafich, G. Y. Robinson, M. M. Al-Jassim, and K. M. Jones, J. Vac. Sci. Technol. B8(2), (1990).
6. M. Razeghi, M. Defour, R. Blondeau, F. Omnes, P. Maurel, O. Acher, F. Brillouet, J.C.C. Fan and J. Salerno, Appl. Phys. Lett. 53, 2389 (1988).
7. J. P. Lorenzo, D. Eirug Davies, and T. G. Ryan, J. Electrochem. Soc. 126, 118 (1979).

(a)



(b)

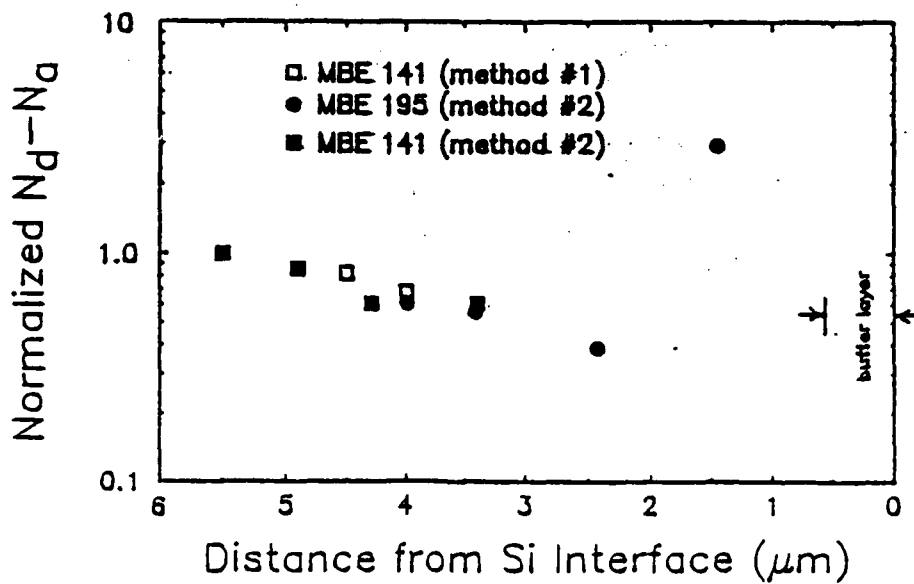


Fig. 1. Variation of room temperature (a) Hall mobility and (b) electron concentration with depth in n-type InP on Si. The normalization procedure is described in the text.

THE BAND OFFSET OF GaAs/In_{0.48}Ga_{0.52}P

Jianhui Chen, J. R. Sites, and I. L. Spain
Department of Physics
Colorado State University
Fort Collins, Colorado 80523

and

M. J. Hafich and G. Y. Robinson
Center for Optoelectronic Computing Systems
and
Department of Electrical Engineering
Colorado State University
Fort Collins, Colorado 80523

ABSTRACT

Low temperature photoluminescence spectra of an In_{0.48}Ga_{0.52}P alloy and a p-type GaAs/In_{0.48}Ga_{0.52}P multiple-quantum well, both grown by molecular beam epitaxy, have been obtained under hydrostatic pressures from 0-6 GPa. The zero-pressure extrapolation of the InGaP(X) to GaAs(Γ) transitions yields a 0.40 ± 0.02 valence band offset, and hence only a small, 0.06 ± 0.02 eV, conduction-band offset. These offset values are in agreement with measured values of the confinement energy versus well-width.

PACS: 62.50.+p, 73.20.Dx, 78.55.Gr

Quantum well structures of GaAs and (InGa)P alloys provide alternatives to the GaAs/(AlGa)As system. They have been attractive because of the larger bandgap energy and the possibility that strain-layer superlattice structures can be grown. However, the band offset of this system has been controversial. A theoretical value of the conduction band offset $\Delta E_c = 0.16$ eV was obtained by Harrison¹ for a GaAs/In_{0.5}Ga_{0.5}P interface. Shubinkov-de Haas measurements² have implied $\Delta E_c = 0.39$ eV, capacitance-voltage profiling of GaAs/(In,Ga)P heterojunctions have given $\Delta E_c = 0.24$ eV³ and 0.19 eV,⁴ and deep level transient spectroscopy⁵ has led to $\Delta E_c = 0.20$ eV. Recently, however, Kobayashi et al.⁶ investigated the current-voltage characteristics of a MOCVD-grown InGaP/GaAs heterojunction bipolar transistor and concluded that ΔE_c was ~30 meV. No other determinations of the band offsets for this system have been reported, to our knowledge.

Hydrostatic pressure has been a powerful tool for studying band structures of semiconductors. Recently, Venkateswaran et al.⁷ and Wolford et al.⁸ used photoluminescence spectroscopy at high hydrostatic pressures to determine the band offset of GaAs/AlGaAs quantum wells. It is the most direct method known. The purpose of this communication is to report the first such measurement of the band offset of GaAs/InGaP quantum wells, enabling us to discriminate between the earlier, discordant results.

The samples were grown by gas-source molecular beam epitaxy (MBE) on a (100) semi-insulating GaAs substrate at 520°C.⁹ The multiple-quantum well (MQW) consisted of a 600-nm InGaP buffer layer, a 20-period well with each containing a 5.9-nm layer of GaAs and 23.7-nm layer of $\text{In}_x\text{Ga}_{1-x}\text{P}$, capped with a 45-nm GaAs layer. The composition parameter, x , was determined from x-ray diffraction to be 0.48 ± 0.01 . Lattice mismatch is less than 0.1%. Based on the photoluminescence described below, the InGaP was a disordered alloy. The MQW was uniformly doped p-type with Be to a concentration of $5 \times 10^{16} \text{ cm}^{-3}$. The bulk sample was grown by the same techniques, but was not intentionally doped. It was in the form of a 2.64- μm layer on a GaAs substrate and was weakly n-type with $n \sim 10^{16} \text{ cm}^{-3}$.

The samples were compressed separately in a miniature diamond anvil cell whose design and operation are described in detail elsewhere.^{10,11} Samples were cut to about $200 \times 200 \times 50 \mu\text{m}$, then loaded together with a small ruby chip as the pressure sensor.¹¹ Argon was used as the pressure-transmitting medium. Photoluminescence spectra were excited by the 514.5-nm line of an Ar-ion laser from samples held at 25 K at pressures up to 6 GPa, using standard procedures.¹¹

Figure 1 shows the photoluminescence (PL) transition energies as a function of pressure for the epitaxial $\text{In}_{0.48}\text{Ga}_{0.52}\text{P}$ alloy sample, and the MQW. In this figure the satellite peaks from phonon-assisted transitions have been omitted for clarity. The solid lines are least-square fits. In both the epitaxial alloy sample (representing the PL of a bulk sample), and the MQW the conduction-to-valence band transitions at the zone center (Γ - Γ) increases rapidly with pressure, while the

indirect transitions from X-related conduction states to the valence-band zone-center (Γ) decrease at a slower rate. This type of behavior is universally observed in III-V bulk samples and MQWs. This allows the observed peaks to be identified as illustrated in Fig. 2. The MQW takes a type-II alignment above 2.6 GPa, so that transitions are indirect in both momentum and real space. This has been confirmed from observations of a blue-shift of transition energy with increased laser power.¹²

PL energies at room pressure, and pressure coefficients are listed in Table 1. The PL energy for the MQW gives good agreement with the bandgap of GaAs when (1) the quantum confinement energy, $E_{1hh} + E_{1e}$ (44 meV for the present MQW, as discussed below), (2) the exciton energy E_{ex} of -5 meV,¹³ (3) Stark energy, E_s of -4 meV,^{14,15} and (4) the Be acceptor energy, E_A of -28 meV¹⁶ are taken into account. The bandgap was found to be 1.510 ± 0.003 eV.

Using Fig. 2, it is straightforward to see that the valence-band offset of this quantum well structure is given approximately as the difference between extrapolated values of X-related transitions, as shown in Fig. 1. ΔE_v thus takes the approximate value of $E_2(0) - E_5(0) = 0.41$ eV. This value needs to be modified to take into account the above corrections. The formula for the valence-band offset becomes (using notation of Fig. 2):

$$\Delta E_v = E_2(0) - E_5(0) + E_{1hh} - E_A$$

where E_{ex} and E_s approximately cancel in the InGaP and GaAs components. Thus, the valence-band offset is modified by the correction due to $E_{1hh} = 15$ meV and $E_A = 28$ meV to:

$$\Delta E_v = (0.40 \pm 0.02) \text{ eV}$$

The conduction-band offset can be determined in a straightforward way from this:

$$\Delta E_c = E_g(\text{InGaP}) - E_g(\text{GaAs}) - \Delta E_v = (0.06 \pm 0.02) \text{ eV}$$

Therefore, Q_c and Q_v , the fractional offsets take the values 0.13 ± 0.04 and 0.87 ± 0.04 .

A consistency check on the large valence band offset can be made by examination of confinement energy as a function of well thickness. Figure 3 shows the total confinement energy, $E_{1hh} + E_{1e}$, previously deduced by PL from a series of quantum wells of varying thickness in a single sample.¹⁷ The calculated thickness dependence of confinement energy for several reported values of ΔE_c and ΔE_v is shown for comparison. Larger ratios of ΔE_v to total offset require thinner wells to yield the same $E_{1hh} + E_{1e}$ since the heavy hole mass term E_{1hh} increases slowly and becomes more dominant. The experimental data clearly agrees better with the calculations where the major portion of the band offset is in the valence band.

The pressure coefficients for all the PL peaks are listed in Table 1. The coefficients for the GaAs(X- Γ) and InGaP(X)-to-GaAs(Γ) transitions are $-(20 \pm 3)$ meV/GPa and $-(30 \pm 3)$ meV/GPa, respectively. The higher value of the latter is somewhat unusual. It may be due to residual stress or to a small shift of the band-offset with pressure. It is noted that the extrapolation of the transition energies to $P = 0$ in the present work estimates the offset at zero-pressure, where this

quantity is of technological interest. Uncertainty in the slope of E_5 , as seen in Fig. 1, make only a small difference in the zero pressure intercept.

In conclusion, photoluminescence spectroscopy was performed on a MBE-grown $\text{In}_{0.48}\text{Ga}_{0.52}\text{P}$ alloy and a $\text{GaAs}/\text{In}_{0.48}\text{Ga}_{0.52}\text{P}$ superlattice at 25 K under hydrostatic pressures. The observation of transitions associated with X-states in bulk InGaP, and both PL components of the GaAs/InGaP MQW, enables a straightforward extrapolation of the band energy separations, so that the band offset of the GaAs/InGaP quantum wells studied can be determined directly. Only 13% of the total band offset is found to occur in the conduction band.

The authors acknowledge the support of the Air Force Office of Scientific Research (contract 89-0513) and the Center for Optoelectronic Computing Systems, sponsored by the National Science Foundation/Engineering Research Center grant CDR2-22236 and by the Colorado Advanced Technology Institute, an agency of the State of Colorado.

REFERENCES

1. W. A. Harrison, J. Vac. Sci. Tech. 14, 1016 (1977).
2. K. Kodama, M. Hoshino, K. Kitahara, M. Takikawa, and M. Ozeki, Jpn. J. Appl. Phys. 25, L125 (1986).
3. M. A. Rao, E. J. Caine, H. Kroemer, S. I. Long, and D. I. Babic, J. Appl. Phys. 61, 643 (1987).
4. M. O. Watanabe, J. Yoshuda, M. Mashita, T. Nakanisi, and A. Hojo, J. Appl. Phys. 57, 5340 (1985).
5. D. Biswas, N. Debbas, P. Bhattacharya, M. Razeghi, M. Defour, and F. Omnes, Appl. Phys. Lett. 56, 833 (1990).
6. T. Kobayashi, K. Taira, F. Nakamura, and H. Kawai, J. Appl. Phys. 65, 4898 (1989).
7. U. Venkateswaran, M. Chandrasekhar, H. R. Chandrasekhar, B. A. Vojak, F. A. Chambers, and J. M. Meese, Phys. Rev. B33, 8416 (1986).
8. D. J. Wolford, T. F. Kuech, and J. A. Bradley, J. Vac. Sci. Instrum. B4, 1043 (1986).
9. H. Y. Lee, M. D. Crook, M. J. Hafich, J. H. Quigley, G. Y. Robinson, D. Li, and N. Otsuka, Appl. Phys. Lett. 55, 2322 (1989).
10. D. J. Dunstan and W. Scherrer, Rev. Sci. Instrum. 59, 627 (1988).
11. D. J. Dunstan and I. L. Spain, J. Phys. E: Sci. Instrum. 22, 913 (1989) and 22, 923 (1989).
12. J. Chen, D. Patel, J. R. Sites, I. L. Spain, M. J. Hafich, and G. Y. Robinson, accepted by Solid State Commun. (1990).
13. M. Jaros, "Physics and Applications of Semiconductor Microstructures" (John Wiley and Sons, New York, 1981).

14. R. D. Dupuis, R. C. Miller, and M. Petroff, *J. Cryst. Growth* 68, 398 (1984).
15. R. C. Miller, R. D. Dupis, and P. M. Petroff, *Appl. Phys. Lett.* 44, 508 (1984).
16. S. M. Sze, "Physics of Semiconductor Devices" (John Wiley and Sons, New York, 1981).
17. M. J. Hafich, J. H. Quigley, R. E. Owens, G. Y. Robinson, D. Li, and N. Otsuka, *Appl. Phys. Lett.* 54, 2686 (1989).
18. C. Alibert, G. Bordue, A. Laugier, and J. Chevallier, *Phys. Rev. B* 6, 1301 (1972).

Table 1. Photoluminescence zero pressure energies and pressure coefficients. 25 K.

	GaAs/InGaP MQW (MBE 144)	InGaP Alloy (MBE 299)
E_g^Γ (eV)	1.510 ± 0.003	1.970 ± 0.002 ($E_1(0)$)
E_g^X (eV)	1.93 ± 0.01 ($E_4(0)$)	2.26 ± 0.02 ($E_2(0)$)
$E_3(0)$	1.511 ± 0.002	
$E_5(0)$ (eV)	1.85 ± 0.01	
E_{1e} (eV)	0.019	
E_{1hh} (eV)	0.015	
E_A (eV)	0.028	
dE^Γ/dP (meV/GPa)	93 ± 2	84 ± 2
dE^X/dP (meV/GPa)	$-(20 \pm 3)$	$-(20 \pm 2)$
dE_5/dP (meV/GPa)	$-(30 \pm 3)$	
Crossover pressure (GPa)	3.5 GaAs (X- Γ)	2.6 InGaP (X- Γ)

FIGURE CAPTIONS

- Fig. 1. Photoluminescence transition energies as a function of pressure for the bulk (InGa)P sample (open circles) and the GaAs/InGaP MQW (open squares). The full lines are least-squares, linear fits, and the dashed lines are extrapolations.
- Fig. 2. A sketch of the energy levels and PL transitions for (a) epitaxial (bulk) (InGa)P at low pressure, (b) a GaAs/(InGa)P MQW at $P = 0$, and (c) the MQW at $P = 2.7$ GPa.
- Fig. 3. The variation of quantum confinement energy for MQWs of varying well thickness. The open circles are the experimental results,¹⁷ and the lines are the results of calculations (using $m_e = 0.11 m_0$ and $m_h = 0.46 m_0$ for InGaP)¹⁸ with various values of the band offsets: dashed line--present result; curve 1--Kobayashi et al.⁵; curve 2--Harrison¹, curve 3--Watanabe et al.⁴; curve 4--Biswas et al.⁵; curve 5--Rao et al.³; curve 6--Kodama et al.²

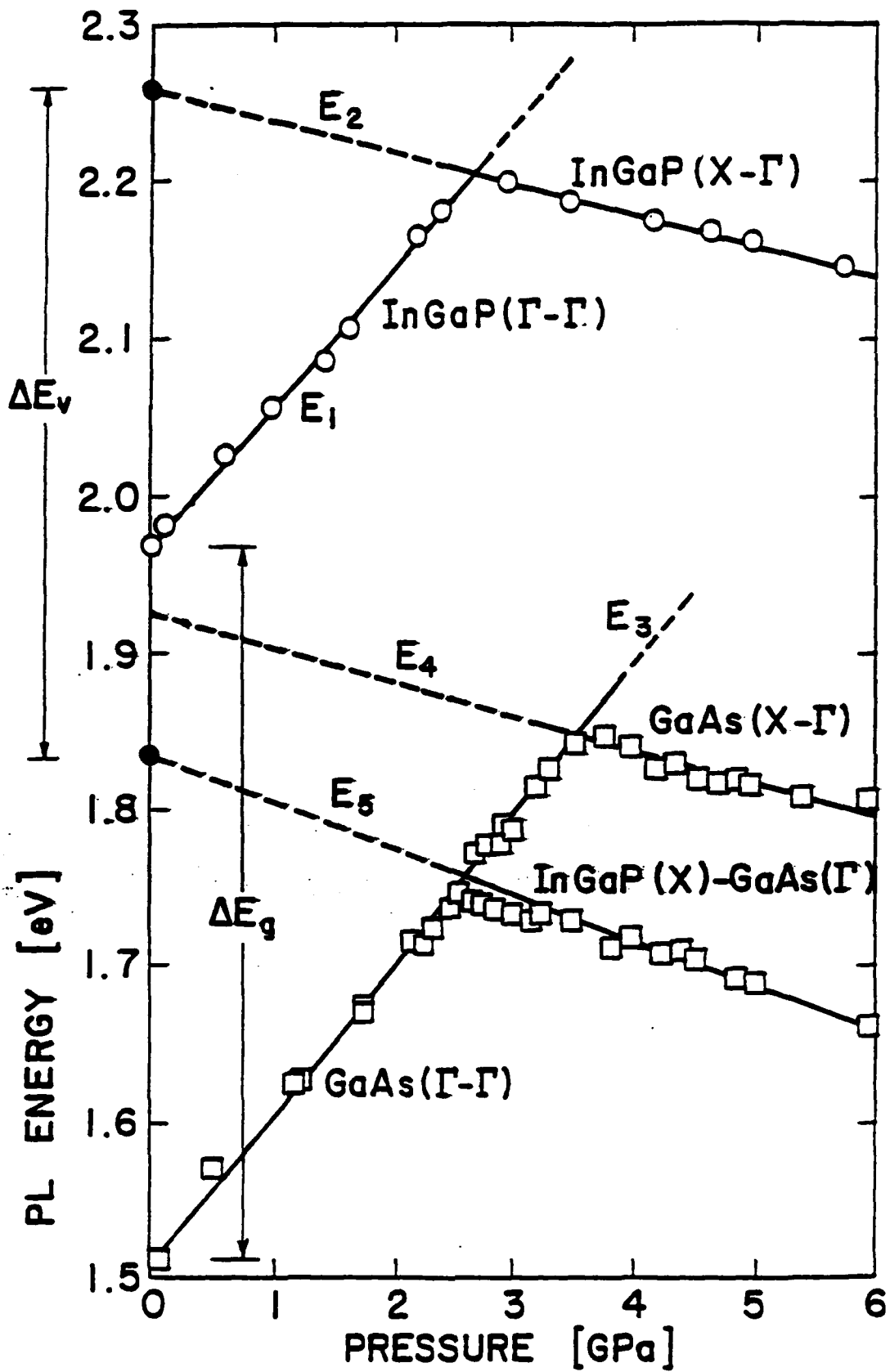


Fig. 1

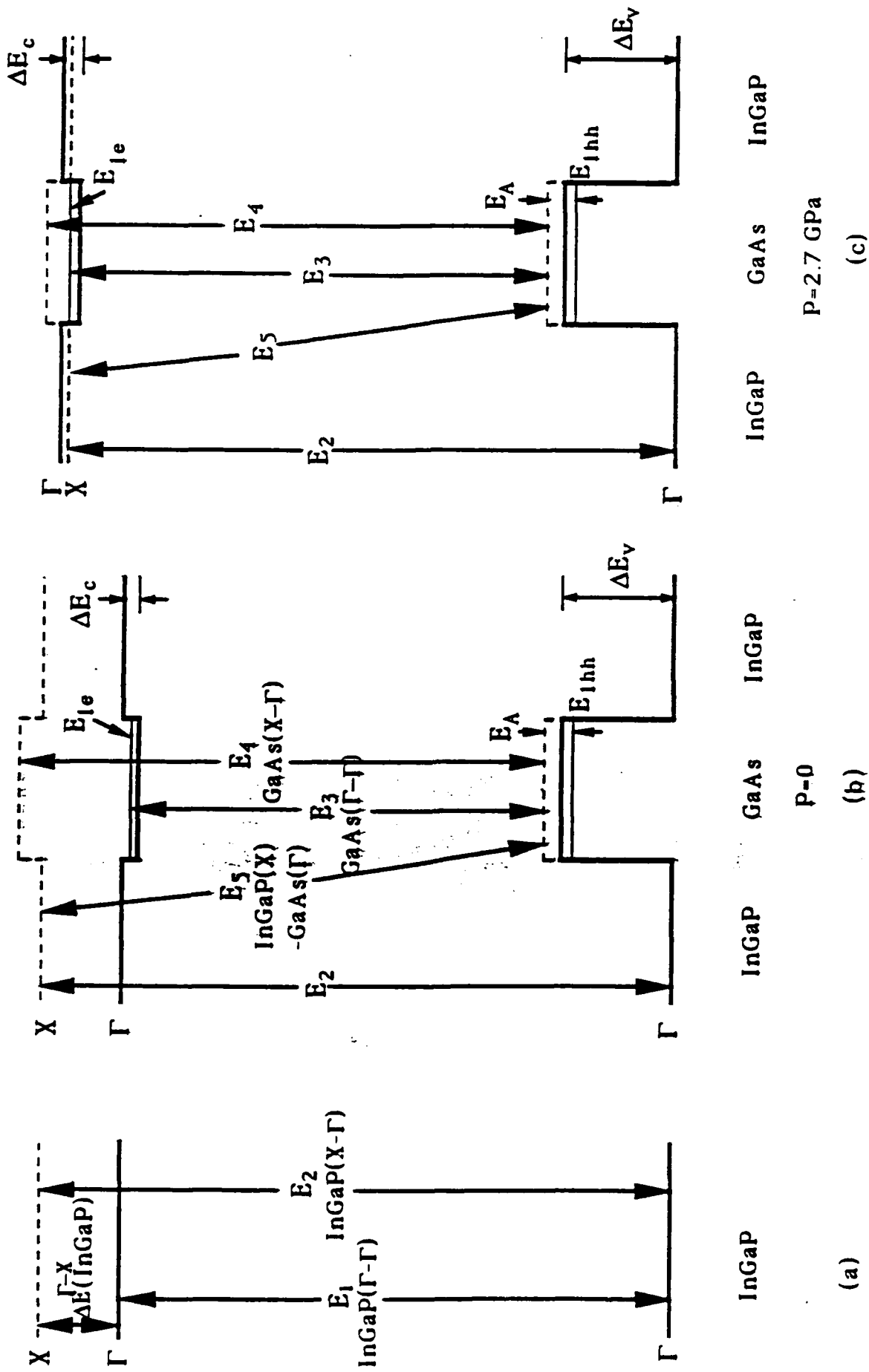


Fig. 2

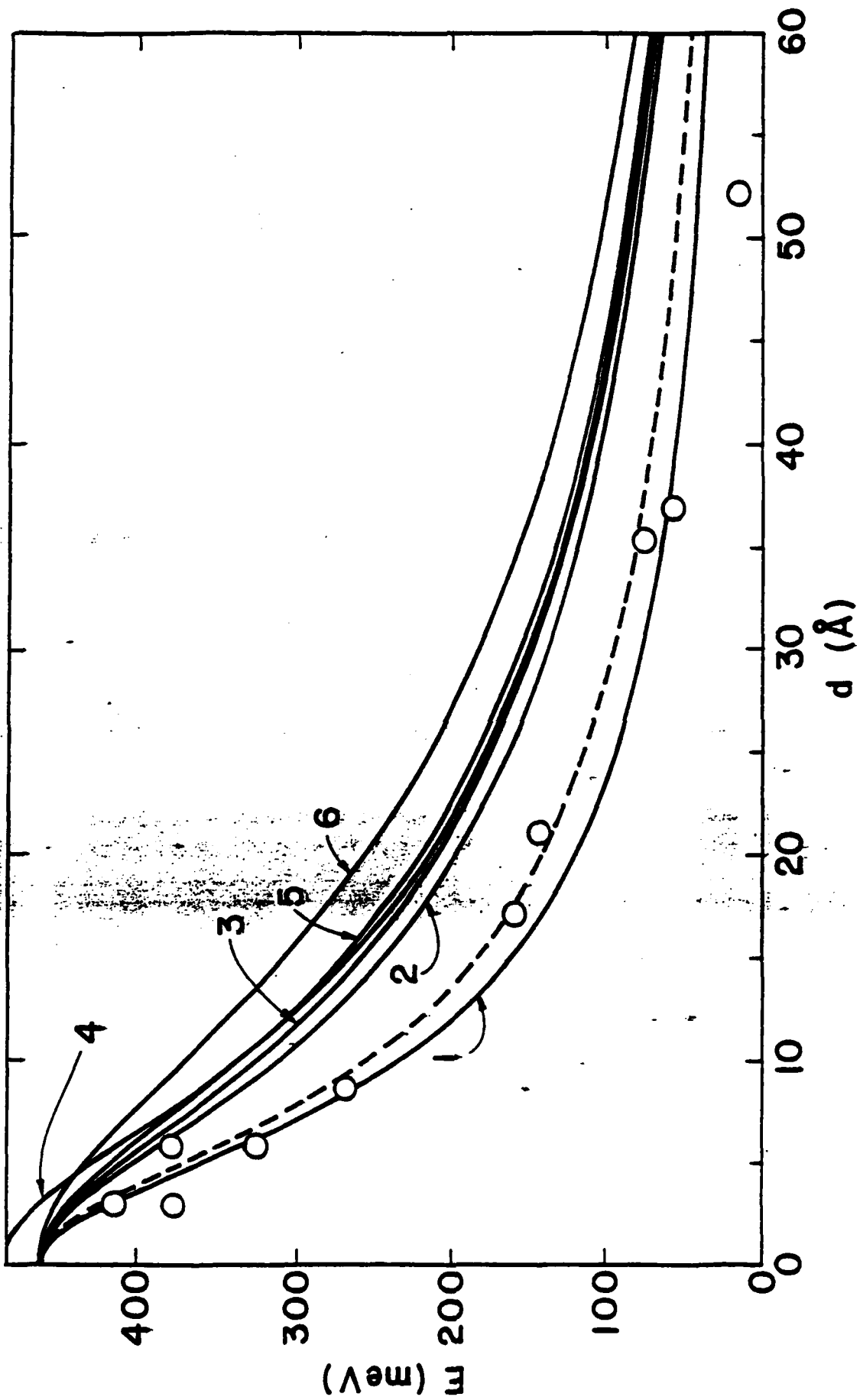


Fig. 3

Internal photoemission and energy band offsets in GaAs-GaInP *pIN* heterojunction photodiodes

M.A. Haase,

3M Company

201-1N-35

3M Center, St. Paul, MN 55144

and

M.J. Hafich, and G.Y. Robinson,

Center for Optoelectronic Computing Systems, and

Electrical Engineering Department,

Colorado State University,

Fort Collins, CO 80523

ABSTRACT

Internal photoemission has been observed in GaAs-Ga_{0.52}In_{0.48}P *pIN* heterojunction photodiodes grown by gas-source molecular beam epitaxy. Threshold energies associated with this photocurrent mechanism have been accurately measured. Simple analysis provides a precise determination of the energy band discontinuities in this heterostructure material system. The results indicate a conduction band discontinuity of $\Delta E_c = 108 \pm 6$ meV at room temperature.

The GaAs-AlGaInP lattice-matched material system is important for the fabrication of visible light emitting devices, and has attracted interest for heterojunction bipolar transistor applications. One of the most important pieces of information needed for understanding the behavior of devices made in this, or any heterostructure material system is the alignment of the energy band extrema. Such information may be extracted by a variety of indirect methods. Reports of measured values for the conduction band discontinuity, ΔE_c , at GaAs-GaInP heterointerfaces range from 30 to 390 meV. The techniques used include Kroemers's C-V technique (190, 220 meV)^{1,2}, deep level transient spectroscopy of quantum wells (198 meV)³, and analyses of two-dimensional electron gases (390 meV)⁴ and heterojunction bipolar transistors (30 meV)⁵.

One of the most direct techniques available for studying band offsets is the analysis of internal photoemission in pN heterojunctions.^{6,7} We have fabricated GaAs-GaInP pIN heterojunction photodiodes and measured the internal photoemission at the heterointerface. The epitaxial layers were grown by gas-source molecular beam epitaxy (GSMBE)⁸. The growth schedule began with a buffer layer of n -GaAs on an n^+ -GaAs substrate, followed by a 1.0 μm thick layer of $\text{Ga}_{0.52}\text{In}_{0.48}\text{P}$. The first 0.2 μm of this $\text{Ga}_{0.52}\text{In}_{0.48}\text{P}$ layer was doped n -type with Si, the remainder being unintentionally doped. The top layer was 0.1 μm of p^+ -GaAs, doped to $p=3\times 10^{18} \text{ cm}^{-3}$ with Be. The sample exhibited nearly perfect morphology and a narrow linewidth (25 arcsec) in double crystal X-ray measurements using the (400) reflection. Room temperature photoluminescence exhibited a peak at 1.885 eV. Diodes were fabricated by evaporating Ti-Au contacts and mesa etching. Capacitance-voltage measurements of the

finished diodes showed that the unintentionally doped GaInP was fully depleted at zero bias.

The spectral response of these devices was measured with standard lock-in amplifier techniques. A tungsten-halogen light source and grating monochromator were used with careful attention to the application of optical filters to minimize higher-order and stray light. A beam splitter was used to illuminate a reference detector while an optical fiber guided the rest of the light to the sample. The entire system is fully computer controlled and was calibrated with a Si photodiode standard. Subsequently, the computer was used to compensate for the spectral characteristics of the optics and the reference detector.

The spectral response of a typical GaAs-GaInP photodiode is shown in Fig. 1. This data was taken at room temperature and zero bias with the light incident on the top (the thin p^+ -GaAs layer). Three distinct regimes are visible in this data. At photon energies, $h\nu$, greater than the band gap of the GaInP (1.885 eV) the quantum efficiency is constant at about 0.5. At energies less than 1.89 eV, the quantum efficiency drops precipitously, and in the range $1.50 < h\nu < 1.85$ eV, it is dominated by internal photoemission. This mechanism is illustrated in the inset of Fig. 1. The photon is absorbed in the p^+ -GaAs layer, stimulating a transition from either the valence band or the acceptor band to a state high in the conduction band. From there, some of these hot electrons surmount the barrier at the GaAs-GaInP interface and are collected, generating photocurrent. The lowest energy photon that can generate photocurrent by this mechanism has energy

$$h\nu_T = E_g - E_A + \Phi, \quad (1)$$

where $h\nu_T$ is the threshold energy, E_g is the band gap energy of GaAs (1.424 eV), E_A is the acceptor ionization energy (28 meV), and Φ is the heterobarrier energy associated with the conduction band discontinuity; $\Phi \approx \Delta E_c$. The actual height of the heterobarrier is slightly less than ΔE_c due to barrier lowering effects which include band bending in the GaAs, image force, and tunneling. These small corrections are considered below.

At photon energies below the threshold energy (about 1.5 eV), the quantum efficiency is dominated by absorption in the GaAs layer and subsequent thermionic emission of some of the photogenerated electrons over the heterobarrier. As expected, the strength of this mechanism decreases precipitously at photon energies below the GaAs band gap energy as the absorption becomes negligible.

In order to obtain a value for ΔE_c from such data, one must accurately determine the threshold energy. The first step is to fit a line to the background thermionic emission at photon energies below threshold, and subtract that component from the photoresponse. Then, using the standard analysis methodology for photoemission experiments, the threshold energy is determined by extrapolation of a power-law fit to the data. In this case, the measured quantum efficiency η was found to very accurately follow the relationship

$$\eta \propto (h\nu - h\nu_T)^3. \quad (2)$$

In Fig. 2, the threshold energy is determined by extrapolations of linear fits to $\eta^{1/3}$ for different values of reverse bias. The precision and reproducibility of these measurements are remarkable. Variations in $h\nu_T$ from diode to diode are consistently less than ± 3 meV.

The heterobarrier energy Φ may be directly calculated from Eq. 1. Figure 3 presents measured barrier heights as a function of reverse bias.

The slight decrease in Φ with increasing reverse bias is indicative of the various barrier lowering effects. The conduction band discontinuity ΔE_c is simply the value of Φ for $V+V_{bi}=0$ (the flat-band condition, where V is the reverse bias voltage and V_{bi} is the built-in voltage.). The curved line in Fig. 3 represents the result of a simple model that accounts for the barrier lowering effects of band bending, image force, and hot electron tunneling. Excellent agreement with the data is achieved for $\Delta E_c=108$ meV. At zero bias, the combined barrier lowering effects total 23 meV.

Because the results of this experiment indicate a value of ΔE_c that is generally lower than previous reports, a comment is in order. With the internal photoemission technique, there are two mechanisms that could conceivably lead to erroneously *low* values of ΔE_c . The first is interface grading.⁶ However, in our experiment, the electric field in the diodes is so low at the interface (17 kV/cm at zero bias) that the grading would have to extend over 500 Å to explain the 100 meV discrepancy between the present results and some of the previous reports. Studies of similar GaAs-GaInP interfaces have shown them to be abrupt on a monolayer (3 Å) scale.⁹ The other conceivable source of error is positive interface charge. In this case, an interface defect concentration of 10^{12} cm⁻² (which is virtually unheard-of at high quality lattice-matched interfaces), would cause only a 24 meV error, due to band bending in the p^+ -GaAs. Either of these potential problems would affect the excellent agreement between the results of the barrier lowering model and experiment. We therefore estimate the uncertainty of our value of ΔE_c to be ± 6 meV, based on experimental precision and the estimated width of the acceptor band.

In conclusion, analysis of internal photoemission in GaAs-GaInP pIN heterojunction photodiodes has provided very precise measurements of

the band offsets. The results indicate $\Delta E_c = 108 \pm 6$ meV at room temperature. Therefore, using a value of 1.885 ± 0.005 eV for the band gap of GaInP we infer that ΔE_v , the valence band offset, is 353 ± 11 meV.

The authors acknowledge helpful discussions with D.K. Misemer, and thank K.A. Gleason for performing the photoluminescence measurements. The work at Colorado State University is supported by the Air Force Office of Scientific Research (contract 89-0513) and the Center for Optoelectronic Computing Systems, sponsored by the National Science Foundation/Engineering Research Center grant CDR-22236 and by the Colorado Advanced Technology Institute, an agency of the State of Colorado.

REFERENCES

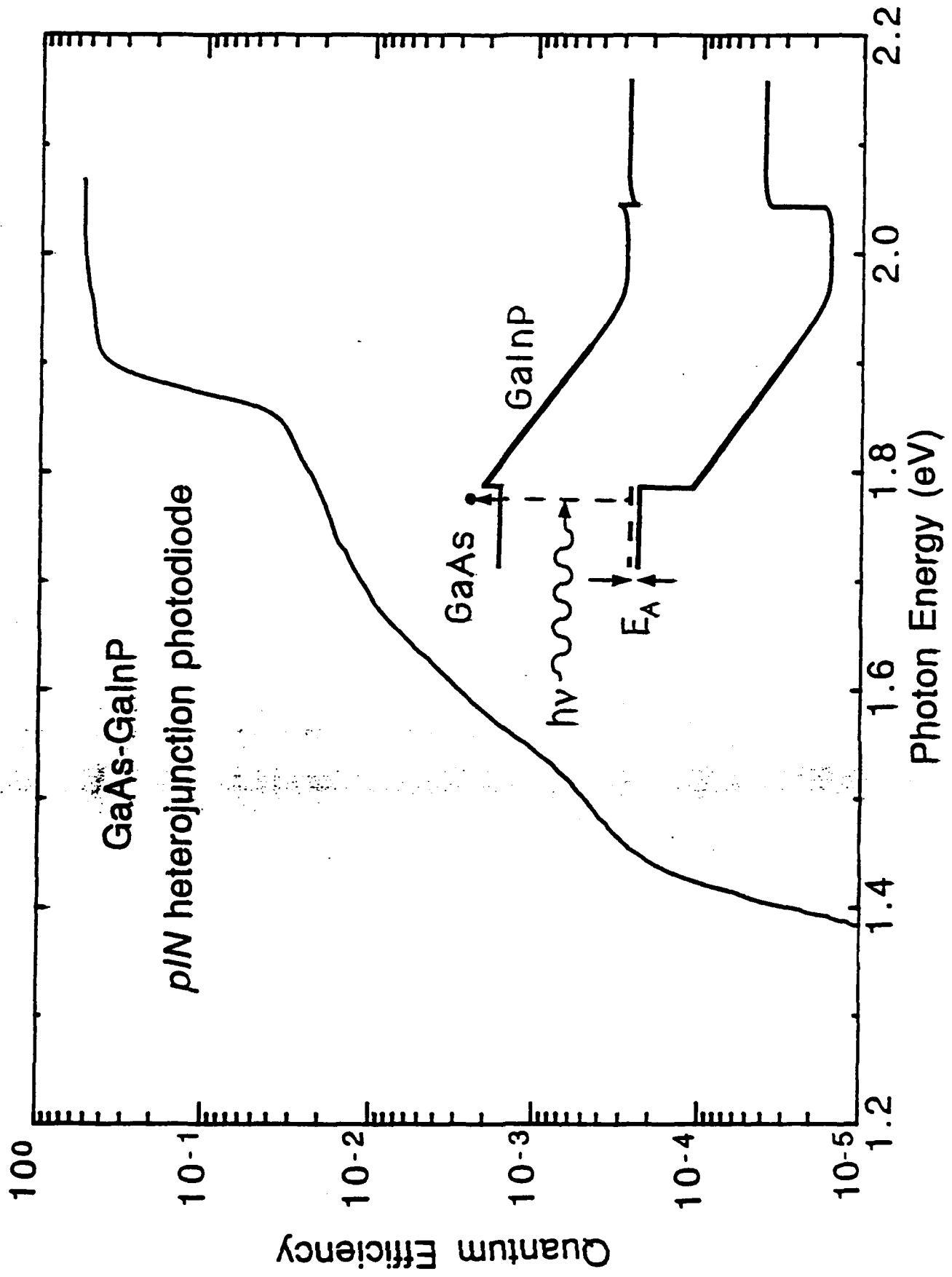
1. M.A. Rao, E.J. Caine, H. Kroemer, S.I. Long, and D.I. Babic, *J. Appl. Phys.* **61**, 643 (1987).
2. M.O. Watanabe and Y. Ohba, *Appl. Phys. Lett.* **50**, 906 (1987).
3. D. Biswas, N. Debbar, P. Bhattacharya, M. Razeghi, M. Defour, and F. Omnes, *Appl. Phys. Lett.* **56**, 833 (1990).
4. K. Kodama, M. Masataka, K. Kitahara, M. Takikawa, and M. Ozaki, *Japan. J. Appl. Phys.* **25**, L127 (1986).
5. T. Kobayashi, K. Taira, F. Nakamura, and H. Kawai, *J. Appl. Phys.* **65**, 4898 (1989).
6. M.A. Haase, N. Pan, and G.E. Stillman, *Appl. Phys. Lett.* **54**, 1457 (1989).
7. M.A. Haase, M.A. Emmanuel, S.C. Smith, J.J. Coleman, and G.E. Stillman, *Appl. Phys. Lett.* **50**, 404 (1987).
8. J.H. Quigley, M.J. Hafich, H.Y. Lee, R.E. Stave, and G. Y. Robinson, *J. Vac. Sci. Technol.* **B7**, 358 (1989).
9. M.J. Hafich, J.H. Quigley, R.E. Owens, G.Y. Robinson, D. Li, and N. Otsuka, *Appl. Phys. Lett.* **54**, 2686 (1989).

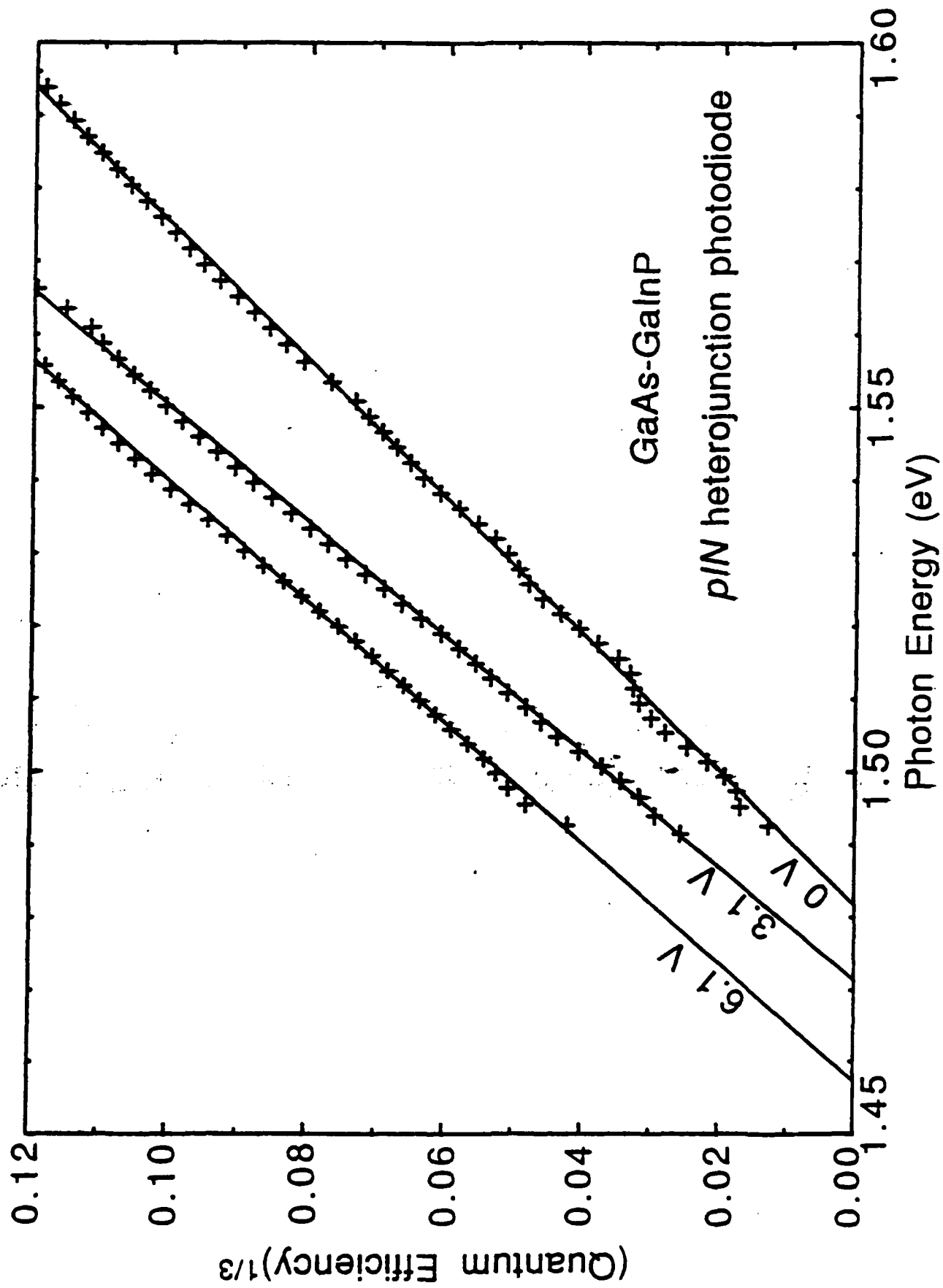
FIGURE CAPTIONS

Fig. 1. The measured spectral response of a GaAs-GaInP *pIN* diode. The inset is a band diagram showing the internal photoemission process.

Fig. 2. Power-law fits to the quantum efficiency of the internal photoemission at various reverse bias voltages.

Fig. 3. Variation of the conduction band heterobarrier energy as a function of reverse bias voltage ($V+V_{bi}$), where V_{bi} is the built-in voltage of the diode. The curved line is the result of a model accounting for barrier lowering effects.





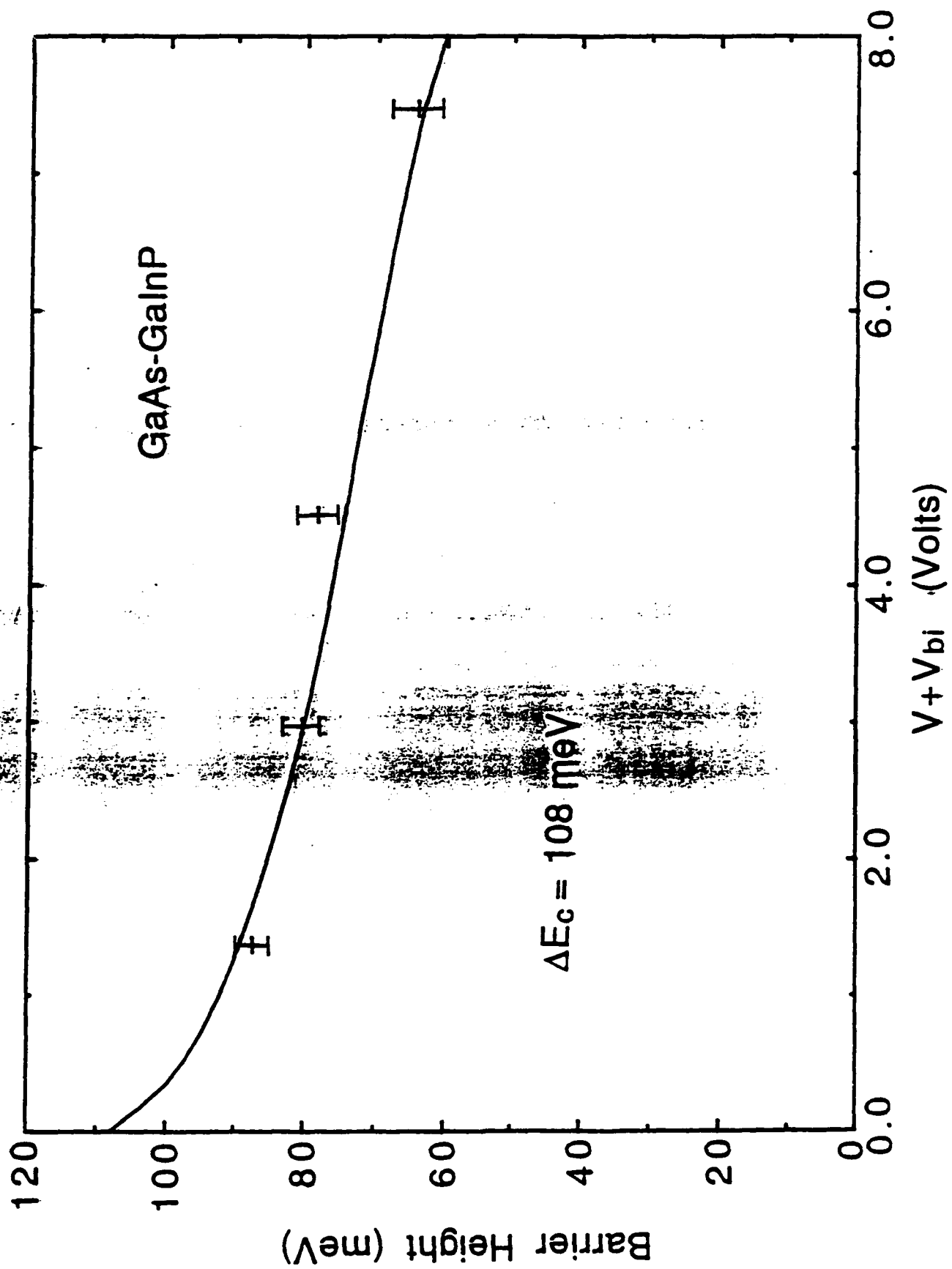


Fig. 3

Presented the Electronic Materials Conference, University of California, Santa Barbara, CA, June 27-29, 1990.

9: 20 AM, E3

Quantum-Confined Stark Effect in InGaP/GaAs Multiple Quantum Wells: G. A. Patrizi, D. G. Wu, M. J. Hafich, H. Y. Lee, P. Silvestre, and G. Y. Robinson, Center for Optoelectronic Computing Systems and Department of Electrical Engineering, Colorado State University, Ft. Collins, CO 80523.

High speed optical modulators using electroabsorption in AlGaAs/GaAs multiple quantum wells (MQW) have been widely reported. The modulation results from the quantum-confined Stark effect (QCSE) shift in the exciton energy level with an applied electric field. The energy shift depends on the proximity of the electronic wavefunction to the bottom of the quantum well. By decreasing the bandedge discontinuity between the well and barrier materials, the wavefunction will move closer to the bottom of the well and the Stark shift will be increased. The lattice-matched InGaP/GaAs system exhibits a lower conduction band discontinuity than the AlGaAs/GaAs system, and thus offers the possibility of larger QCSE modulation for heterostructures with the same well thickness and applied field. We report here the first measurements of optical absorption in InGaP/GaAs MQW structures.

In_{0.48}Ga_{0.52}P/GaAs MQW p-i-n heterostructures were grown on n⁺(100) GaAs substrates using gas-source molecular beam epitaxy. Each sample consisted of a thick n⁺ InGaP buffer layer covered by an unintentionally doped (n ~ 3x10¹⁶cm⁻³) MQW region consisting of 20-50 periods of 100-Å GaAs wells and 100-Å InGaP barriers, and capped by a thin p⁺ InGaP layer. Lattice mismatch and layer thicknesses were determined by double crystal x-ray diffraction. P-i-n diodes, fabricated using mesa etching and conventional metallization techniques, exhibited low dark currents (< 5 nA) and breakdown voltages of over 30V.

Room temperature photocurrent spectra at zero bias showed the expected absorption edge with clearly resolved excitonic resonances for the n = 1 heavy and light hole transitions and the n = 2 heavy hole transition. Initial results demonstrate that the absorption edge shifts to lower energy with increasing reverse bias. Theoretical calculations indicate that for a GaAs well of 100Å in thickness at a field of 10⁵V/cm, an In_{0.48}Ga_{0.52}P barrier should produce a QCSE shift over 50% larger than that produced by an Al_{0.32}Ga_{0.68}As barrier.